HHS Public Access

Author manuscript

ACS Chem Neurosci. Author manuscript; available in PMC 2021 July 01.

Published in final edited form as:

ACS Chem Neurosci. 2020 July 01; 11(13): 2019–2030. doi:10.1021/acschemneuro.0c00324.

Targeting nitric oxide production in microglia with novel imidazodiazepines for non-sedative pain treatment

Amanda N. Nieman[a], **Guanguan Li**[b], **Nicolas M. Zahn**[a], **Md Yeunus Mian**[a], **Brandon N. Mikulsky**[c], **Dylan A. Hoffman**[a], **Taylor M. Wilcox**[a], **Alexander S. Kehoe**[a], **Ian W. Luecke**[a], **Michael M. Poe**[d], **David Alvarez-Carbonell**[e], **James M. Cook**[a], **Douglas C. Stafford**[a,c], **Leggy A. Arnold**[a,c,*]

[a]Department of Chemistry and Biochemistry and the Milwaukee Institute for Drug Discovery, University of Wisconsin-Milwaukee, Milwaukee, Wisconsin 53201, United States

[b]Shenzhen Grubbs Institute and Department of Chemistry, Shenzhen Key Laboratory of Small Molecule Drug Discovery and Synthesis, Southern University of Science and Technology, Shenzhen, Guangdong 518055, China

[c]Pantherics Incorporated, La Jolla, California 92037, United States

[d]Department of Chemistry, Western Michigan University, Kalamazoo MI 49008, United States

[e]Department of Molecular Biology and Microbiology, Case Western Reserve University, Cleveland, Ohio 44106, United States

Abstract

The goal of this research is the identification of new treatments for neuropathic pain. We characterized the GABAergic system of immortalized mouse and human microglia using electrophysiology and qRT-PCR. Cells from both species exhibited membrane current changes in response to γ-aminobutyric acid, with an EC_{50} of 260 nM and 1940 nM, respectively. Human microglia expressed high levels of the γ-aminobutyric acid type A receptor ($GABA_AR$) α_3 subunit, which can assemble with β_1 and γ_2/δ subunits to form functional $GABA_ARs$. Mouse

*Corresponding Author, Department of Chemistry and Biochemistry, University of Wisconsin-Milwaukee, Milwaukee, WI 53201, arnold2@uwm.edu.

Author Contributions

L.A.A. and D.C.S. conceived the project. L.A.A. and D.C.S. were responsible for the overall experimental design with input from J.M.C. A.N.N., N.M.Z., B.N.M., D.A.H., T.M.W., A.S.K. and I.W.L. performed the described experiments. D.A.-C. provided the mouse and human microglia cell lines and proved valuable input in regards to their culture conditions. G.L., M.Y.M. and M.M.P. synthesized the investigated small molecules. A.N.N. and L.A.A. wrote the manuscript with input from all authors.

Supporting Information

The Supporting Information is available free of charge at: https://pubs.acs.org

Structures of all compounds, concentration dependent reduction of NO for most active compounds, viability data for HEK293 and HEPG2 cells, PDSP screening data for MP-IV-010, primer sequences for mouse and human $GABA_AR$ subunits.

Conflict of Interest

The compounds disclosed in the publication are disclosed in the following patents. Dr. Cook in: “Selective Agents for Pain Suppression” (US20100317619), “Stereospecific Anxiolytic and Anticonvulsant Agent with Reduced Muscle-Relaxant, Sedative, Hypnotic, and Ataxic Effects” (US20060003995), “Anxiolytic Agents with Reduced Sedative and Ataxic Effects” (US7119196B2) and “GABAergic Agents to Treat Memory Deficits” (US20100130479). Drs. Cook and Li are inventors of patents: “GABAergic Ligands and Their Uses” (WO2016154031) and “Treatment of Cognitive and Mood Symptoms in Neurodegenerative and Neuropsychiatric Disorders with Alpha-5-containing GABA(A) receptor Agonists” (WO2017161370). Drs. Li, Cook, Stafford and Arnold are inventors of patent “GABA(A) Receptor Modulators and Methods to Control Airway Hyperresponsiveness and Inflammation in Asthma” (WO2018035246A1).

microglia contained α_2, α_3 and α_5, in addition to $\beta_{1–3}$, $\gamma_{1–2}$ and δ, mRNA, enabling a more diverse array of $GABA_AR$s than human microglia. Benzodiazepines are well-established modulators of $GABA_AR$ activity, prompting a screen of a library of diverse benzodiazepines in microglia for cellular effects. Several active compounds were identified by reduction of nitric oxide (NO) in interferon gamma and lipopolysaccharide activated microglia. However, further investigation with $GABA_AR$ antagonists flumazenil, picrotoxin, and bicuculline demonstrated that $GABA_AR$s were not linked to the NO response. A screen of 48 receptors identified the κ-opioid receptor and to a lesser extent the μ-opioid receptor as molecular targets, with opioid receptor antagonist norbinaltorphimine reversing benzodiazepine induced reduction of microglial NO. Functional assays identified the downregulation of inducible NO synthase as the mode of action of imidazodiazepines MP-IV-010 and GL-IV-03. Like other κ-opioid receptor agonists, GL-IV-03 reduced the agitation response in both phases of the formalin nociception test. However, unlike other κ-opioid receptor agonists, MP-IV-010 and GL-IV-03 did not impair sensorimotor coordination in mice. Thus, MP-IV-010 and GL-IV-03 represent a new class of non-sedative drug candidates for inflammatory pain.

Keywords

microglia; $GABA_AR$; benzodiazepine; nitric oxide; opioid receptor; formalin test

Introduction

Neuropathic pain (NP) is a difficult to treat type of chronic pain occurring in about 7% of the US population[1]. This chronic pain can arise without overt stimulation of associated peripheral sensory endings and is commonly associated with diabetic neuropathy, HIV infection, post-herpetic neuralgia, and chemotherapy treatment for cancer.[2] While previously thought to simply function as a scaffold for the neuronal networks, more recent evidence suggests glia contribute to neurological disorders, such as Alzheimer's disease, autism, and chronic pain.[3, 4] At the front line of immune defense in the central nervous system (CNS) are resident macrophages, the microglia that have been implicated in many neuro-inflammatory diseases such as Alzheimer's disease, Parkinson's disease, multiple sclerosis, and neuropathic pain.[5] Upon nerve injury, microglia are activated by extracellular adenosine 5′-triphosphate (ATP) released from damaged cells.[6] ATP binds to purinergic receptors, particularly P2X4Rs, which are calcium permeable and promote calcium entry into the cell.[7] The increase in intracellular calcium promotes neuro-inflammation via the release of mediators, such as cytokines, various chemokines, and cytotoxic compounds; substances known to contribute to allodynia, hyperalgesia, and nociception.[8–10] One such cytotoxic compound is nitric oxide (NO), synthesized by nitric oxide synthase (NOS) through the conversion of L-arginine to L-citrulline.[11, 12] During inflammation, large amounts of NO are released into the spinal cord, which sensitizes neurons, reduces firing thresholds, and increases neuronal firing leading to painful sensations.[11] Confirming the role NO plays in pain, direct injection of NO causes pain and NOS inhibitors have exhibited analgesic activity.[11] Among the three isoforms of NOS (neuronal, endothelial, and inducible or iNOS), iNOS is expressed in immune cells, such as macrophages, and it is the only form of NOS to be reported in microglia.[13] Microglial activation induces the expression of iNOS that in turn

produces large cytotoxic quantities of NO. Functional γ-aminobutyric acid type A receptors ($GABA_AR$), which are well-characterized in neurons, have recently been discovered in microglia.[14] These heteropentameric membrane chloride channels are commonly arranged as alternating α, β, and γ subunits.[15, 16] In addition, α and β subunits alone can form functional receptors.[17] Currently, only $α_1$, $α_3$, and $β_1$ subunits have been described in mouse microglia.[14] It has been demonstrated that microglia $GABA_ARs$ can mediate immune suppressive signaling.[18] Previous *in vivo* studies have shown reduced alveolar macrophage numbers in ovalbumin sensitized and challenged mice treated orally with novel $GABA_AR$ positive allosteric modulators.[19, 20] There is evidence that resident macrophage populations, including alveolar macrophages and microglia, arise early in development from common progenitors in the yolk sack distinct from circulating macrophage precursors.[21] Additionally, previous research with α2/α3-subtype $GABA_AR$ positive allosteric modulators has shown these novel imidazodiazepines to be analgesic.[22,23] Taken together, these studies support the use of novel imidazodiazepines in targeting microglia-mediated inflammation as a therapeutic approach to treat neuropathic pain.

Results

To verify the expression of functional $GABA_AR$ on immortalized microglia, cells were patch clamped at −80 mV and current responses acquired for 3 second applications of increasing concentrations of GABA (Figure 1).

Commercially available HMC3 cells exhibited a robust current change in the presence GABA (Figure 1, B). During the GABA application, the negative current increased followed by a rapid recovery once GABA was washed away with external cellular solution. Automated patch clamp technology enabled recording of the average signal of twenty patch clamped cells simultaneously and conducting experiments with eight independent microfluidic systems on the same plate. Average current sweeps are depicted in Figure 1, B. The data were normalized to the maximum negative current response recorded for 1 mM GABA (746 pA). The time dependent currents resulted an EC_{50} value of 270 nM for GABA (Figure 1, A). Literature reports have called into question if HMC3 cells (also called CHME-5 cells) are truly of human origin.[24] Accordingly, additional immortalized human and mouse microglia cell lines were obtained from Case Western Reserve University (Cleveland, OH).[24] Both cell lines were cultured and analyzed with patch clamp as described for HMC3 cells (Figure 1, C and D). The maximum current response for 1 mM GABA was 1245 pA for the human and 1514 pA for the mouse cells. GABA concentration dependent studies established an EC_{50} of 260 nM and 1940 nM for the mouse and human microglia, respectively (Figure 1, C). RT-PCR was used to determine the expression of $GABA_AR$ subunits in human and mouse microglia (Figure 2, B and D), which was compared to corresponding mRNA levels in mouse cerebellum and human brain extract (Figure 2, A and C).

Overall, we observed that the expression of $GABA_AR$ subunits is less pronounced in human microglia than in an extract containing all brain cell types (Figure 2, A and B). For alpha subunits, $α_3$ is the most abundant subunit in human microglia in contrast to $α_1$ in the brain (mostly neurons) (Figure 2, A). Possible binding partners that form functional $GABA_AR$

receptors in human microglia are β_1 and γ_2/δ (Figure 2, B). Mouse microglia did not express α_4 or α_6 $GABA_AR$ subunits, however, α_2, α_3, and α_5 mRNA were observed at similar amounts (Figure 2, D). Other expressed $GABA_AR$ subunits were $\beta_{1–3}$, $\gamma_{1–2}$ and δ. Thus, mouse microglia express a more diverse subset of $GABA_ARs$ than human microglia. This finding supports our earlier observation that GABA induced a current change at a lower concentration in mouse microglia than human microglia.

Next we investigated a library of $GABA_AR$ ligands to identify compounds that reduce the production of NO as a marker of anti-inflammatory activity. Mouse microglia and macrophage line RAW264.7 were activated with interferon gamma (IFNγ) and *E. coli* lipopolysaccharide (LPS), followed by compound exposure at 50 or 10 μM for 24 hours in the presence of 1 μM GABA. NO was quantified with a Greiss assay. Cell viability was determined with CellTiter-Glo. The results are summarized in Table 1.

The screen identified several compounds that reduced NO in activated microglia and macrophages. The tested compounds included achiral and chiral imidazodiazepines and benzodiazepines. In general, microglia were more sensitive to compound treatment with more pronounced reduction of NO than macrophages. The most potent compounds were analyzed at the concentrations indicated in Table 1 and Supporting Information. None of the compounds tested exhibited pronounced toxicity at 50 μM. Cell viability assays with HEK293 (kidney) and HepG2 (liver) cells were conducted in a concentration dependent manner. The percent viability following compound exposure at 120 μM is summarized in Table 1. A limited number of compounds, such as GL-III-63, GL-III-76A, and GL-III-77, were toxic at 120 μM. Most compounds exhibited an LD_{50} >100 μM for both cell lines.

Among the diverse set of compounds, many imidazodiazepines-[1,2,4]-oxadiazoles reduced the NO production by activated microglia. The general structure is depicted in Figure 3.

All active imidazodiazepines-[1,2,4]-oxadiazoles share the pendant 2-fluorophenyl group. Compounds with a 2-pyridine substituent such as GL-II-33 did not reduce NO production. Secondly, a R_2 methyl substituent was superior to a R_2 = H demonstrated by GL-III-23. Thirdly, compounds with a (R) stereochemistry for R_2 = methyl were more active than the corresponding compounds with a (S) configuration. Among the R_3 substituents, the ethyl group was superior to the methyl or isopropyl groups for compounds bearing a bromo or cyclopropyl group in the R_1 position. Among this group GL-IV-03 was the most active compound, reducing NO production by 90% for microglia and 75% in macrophages. For compounds with an acetylene substituent, MP-IV-010 was the most active compound with a R_3 isopropyl group. For both, GL-IV-03 and MP-IV-010, no significant toxicity was observed for microglia and macrophages at 50 μM, however, at 120 μM some cytotoxicity was observed for HEK293 and to a lesser degree for HEPG2 cells.

Three $GABA_AR$ antagonists were used to confirm the activity $GABA_AR$ in MP-IV-010 mediated NO reduction in activated microglia. Antagonists included picrotoxin, which binds within the chloride pore of the receptor, blocking the chloride flux,[15] and bicuculline, which competitively binds at the GABA site of the receptor and prevents endogenous activation.[15] Flumazenil is a direct antagonist of the benzodiazepine site of $GABA_ARs$.[15] For the

competition experiments, microglia were activated with LPS and IFNγ and treated with each antagonist in the presence of MP-IV-010 and GABA. The cell viability for each condition was measured with CellTiter-Glo. The results are summarized in Figure 4 A and B.

Positive control compound dexamethasone reduced NO production of activated microglia without cell toxicity at 100 nM (Figure 4, A). GABA at 1 μM had no effect on the secreted NO levels but significant reduction was demonstrated with MP-IV-010 (50 μM). The administration of 50 μM flumazenil, 50 μM picrotoxin, or 100 μM bicuculline with 50 μM MP-IV-010 did not reverse its NO effects. No cytotoxicity was observed for any treatment conditions (Figure 4, B).

Because reduction of NO could not be reversed by $GABA_AR$ antagonists, we evaluated possible binding of MP-IV-010 to other cellular receptors in collaboration the NIMH Psychoactive Drug Screening Program.[25] Of the 46 receptor competition assays in the screen, MP-IV-010 demonstrated more than 50% activity for only three receptors; confirming the binding to the benzodiazepine site of the $GABA_AR$, but also binding to the κ-opioid receptor and the σ2 receptor (for all results see Supporting Information). To determine the affinity of MP-IV-010 for these receptors, concentration dependent assays were carried out as depicted in Figure 5.

Our results demonstrated MP-IV-010 binding to the benzodiazepine site of $GABA_ARs$ with an affinity of 2.5 μM (IC_{50}) (Figure 5, A). The most abundant $GABA_AR$ in the rat brain homogenate exhibits the $\alpha_1\beta_{2/3}\gamma_2$ configuration. The affinity for the $\alpha_3\beta_3\gamma_2$ $GABA_AR$ was 14.3 μM (EC_{50}) determined by a membrane potential red dye assay (data not shown). Higher affinity was observed for the κ-opioid receptor with an IC_{50} of 351 nM (Figure 5, B). This binding was selective among other opioid receptors subtypes with 33% and 5% inhibition at 10 μM for the μ- and δ- opioid receptors, respectively (Figure, 5, D). The affinity for the σ2 receptor was 5.2 μM (IC_{50}) (Figure 5, C). Furthermore, the compound gave 29% inhibition at 10 μM for the hERG channel, consistent with low cardiotoxic potential (Figure 5, D).

To validate the possible involvement of κ-opioid and σ2 receptors, we determined if selective κ-opioid receptor antagonist norbinaltorphimine and selective σ2 receptor antagonist SM-21[26] can oppose reduction of NO by MP-IV-010 (Figure 6).[27]

In the presence of SM-21 (30 μM), no reversal of NO production by MP-IV-010 (50 μM) was observed (Figure 6, A). However, norbinaltorphimine (30 μM) reversed the effects of MP-IV-010. Neither treatment reduced cell viability (Figure 6, B).

Next, we investigated the possible involvement of iNOS in MP-IV-010 (and structurally similar compound GL-IV-03) mediated reduction of NO in activated microglia. iNOS activity was measured in activated microglia after a 24 hour treatment with MP-IV-010. Secondly, proteins were harvested from microglia activated for 24 hours with LPS/INFγ followed by a 2 hours treatment with MP-IV-010 before measuring iNOS activity. Finally, mRNA and protein levels were quantified for GL-IV-03 treated activated microglia to examine the transcriptional regulation of iNOS. The results are depicted in Figure 7.

Cellular protein extracts from activated microglia exhibited a significantly higher iNOS activity than extracts from non-activated microglia. MP-IV-010 (50 μM) treatment for 24 h completely inhibited the increased iNOS activity in activated microglia (Figure 7, A). To demonstrate that MP-IV-010 does not inhibit iNOS directly, cellular extracts from activated microglia were incubated with MP-IV-010 for 2 h followed by assay of iNOS activity. Here, iNOS activity did not differ from the vehicle treated cell extract (Figure 7, B). However, *iNOS* mRNA levels were reduced in activated microglia 15, 60, and 180 minutes after GL-IV-03 (10 μM) treatment (Figure 7, C). Interestingly, increased iNOS mRNA levels were observed after 6 h. Nevertheless, the amount of iNOS protein isolated from microglia after a 24 h treatment with GL-IV-03 was significantly lower in comparison to vehicle treated cells (Figure 7, D).

The antinociceptive effect of GL-IV-03 was investigated with the formalin test. Paw injections of formalin elicited a biphasic pain response separated in time (1–5 minutes and 20–60 minutes).[28] Licking and biting of the injured hind paw as a demonstration of nociception was evaluated in comparison to the uninjured contralateral paw. The amount of time attending to this behavior during a five-minute interval for each treatment is presented in Figure 8A. Sensorimotor impairment and sedation were investigated with mice that were trained to balance on a rotating rod over a period of three minutes (rotarod). The amount of time that mice remained balanced on the rod after intraperitoneal (i.p.) and oral (p.o.) treatment with GL-IV-03 and MP-IV-010 is summarized in Figure 8B and C.

GL-IV-03 exhibited antinociceptive effects in both acute pain (phase 1) and inflammation mediated pain (phase 2) when administered orally at 10 mg/kg (Figure 8A). The effect was similar to non-steroidal anti-inflammatory drug ketoprofen at 30 mg/kg. Sedation and inhibition of sensorimotor coordination can influence licking and biting pain behaviors, prompting rotarod studies for GL-IV-03 and MP-IV-010. Both compounds administered p.o. at 4-fold the effective dose in the formalin test did not cause any sensorimotor deficits as measured on the rotarod (Figure 8B). Furthermore, intraperitoneal injections of GL-IV-03 at 10 and 40 mg/kg did not influence the ability of mice to balance on a rotating rod for three minutes (Figure 8C). In contrast to diazepam, a benzodiazepine with high affinity for the $\alpha_1\beta_{2/3}\gamma_2$ and other $GABA_AR$ subtypes, was sedating at 5 mg/kg.

Discussion

Microglia are essential in CNS development/homeostasis and are implicated in numerous neuropsychiatric and neurodegenerative disorders. They mediate neuro-inflammation (or para-inflammation) and contribute to NP.[29] Upon activation from nerve injury, microglia promote neuro-inflammation via the release of mediators including NO contributing to allodynia, hyperalgesia, and nociception.[8] Although $GABA_AR$ α_1, α_3, and β_1 subunits have been reported for human microglia cells derived from the frontal lobe,[14] we expanded this knowledge by demonstrating that α3 is the most abundant $GABA_AR$ subunit in human microglia, capable of forming functional $GABA_AR$ subtypes with β1 and γ2 or δ that respond to GABA with a change of membrane current. The $GABA_AR$ subunit expression for mouse microglia include α_2 and α_5 subunits with $\beta_{1–3}$, $\gamma_{1–3}$ or δ as possible binding partners. We hypothesize that the higher abundance of $GABA_AR$ subunit expression for

rodent microglia (HMC3 were derived from rat glioma) is reflected by induced current change at a lower GABA concentrations. Based on these data, it was predicted that $\alpha_3\beta_{2/3}\gamma_2$ selective $GABA_AR$ ligands can attenuate inflammatory mediators such as NO when microglia are activated with LPS and IFNγ. However, compounds that significantly reduced NO production such as MP-IV-010 exhibited only weak affinity for the $\alpha_1\beta_{2/3}\gamma_2$ and $\alpha_3\beta_{2/3}\gamma_2$ $GABA_AR$ subtypes. The inability to reverse this effect with $GABA_AR$ antagonists confirmed that $GABA_ARs$ do not directly mediate anti-inflammatory effects of MP-IV-010. However, our studies showed that novel active imidazodiazepines exhibited high affinity for the κ-opioid receptor. This is consistent with previous studies by Römer, et al. that reported benzodiazepine tifluadom bound the κ-opioid receptor and exhibited analgesic effects with low dependence potential.[30] The investigation of a library of structural analogs around this compound resulted in the discovery of sub-nanomolar ligands for the κ-opioid receptor.[31, 32] Even midazolam, diazepam, and chlordiazepoxide exhibit micromolar affinities for the κ-opioid receptor.[33] Importantly, κ-opioid receptor antagonist norbinaltorphimine reversed the effects of MP-IV-010, implying that κ-opioid receptors are expressed by microglia, which has been reported by Chao, et al.[34] Furthermore, microglia express μ-opioid receptors.[35] Secondly, it confirmed that activation of the κ-opioid receptor regulates NO production. We have demonstrated that MP-IV-010 does not directly inhibit the enzymatic activity of iNOS, but rather modulates its expression. Similar results have been published with opioid receptor agonist biphalin a dimeric enkephalin that reduced iNOS expression in addition proinflammatory factors such as IL-1β, IL-18, COX-2, and NLRP3 in LPS-treated primary microglial cells.[36] The transcriptional effects were mediated by diminished levels of p-NF-κB, p-IκB, p-p38MAPK, and TRIF that were reversible by opioid receptor antagonist naloxone. Like biphalin, MP-IV-010 interacts with μ-opioid receptor although at higher concentration, thus we cannot exclude the possibility that regulation of iNOS is mediated by both opioid receptors. Finally, we demonstrated that GL-IV-03, a more active NO reducing compound, attenuated the agitation response in both phases of the formalin test. Similar results were observed with κ-opioid receptor agonist (–)U50,488H.[37] κ-opioid receptor agonists dynorphin A and ICI-199.441 also reduced paw flinches in the formalin test for both phases in addition to attenuated tactile allodynia and thermal hyperalgesia in the chronic constriction injury model.[38] The anti-nociception effects were reversible with κ-opioid receptor antagonists naloxone and 6'-guanidinonaltrindole. In contrast to (–)U50,488H, which causes sedation at ≥ 2.5 mg/kg (SC),[39] GL-IV-03 and MP-IV-010 did not induce sensorimotor impairment.

Conclusion

Microglia are compelling targets for the development of new non-sedative pain medications. The reduction of iNOS and other pro-inflammatory mediators induced by LPS/INFγ has identified a select group of imidazodiazepines that mediate their response in part via opioid receptors, but do not cause adverse sensorimotor effects. Future research will characterize the signal transduction of these compounds and enable structure-activity relationship studies to optimize new drug candidates for neuropathic and inflammatory pain.

Methods

Chemicals:

Imidazodiazepines and benzodiazepines were synthesized by the Cook Group according to established protocols. (see Supporting Information)

Animals:

5–10 week old male Swiss Webster mice (Charles River Laboratory, WIL, MA) were housed under specific pathogen-free conditions, under standard conditions of humidity, temperature, and a controlled 12 h light and dark cycle and *ad libidum* access to food and water. All animal experiments were conducted in compliance with the University of Wisconsin-Milwaukee Institutional Animal Care and Use Committee (IACUC).

Cell culture:

A) HMC3 Microglia (CRL-3304) were maintained in treated cell culture flasks (Nunc, 156472) with EMEM (Corning, 10010CV) supplemented with 10% heat-inactivated FBS (Corning, 35011CV) and 100 U/mL penicillin and 100 μg/mL streptomycin (Hyclone, SV30010). Cultures were maintained at 37°C and 5% CO_2. When cells reached a density of 7×10^4 cells/mL, cultures were passaged with 0.25% Trypsin (Corning, 25–053-CI) and resuspended to a density no lower than 10,000 cells/mL. B) Human and mouse microglia cell lines were a gift from Dr. David Alvarez-Carbonell at Case Western Reserve University (Cleveland, OH).[24] Microglia were cultured in cell culture treated flasks (Nunc, 156472) with DME/F12 media (Hyclone, SH30023.01) supplemented with 10% heat-inactivated FBS (Corning, 35011CV), 100 U/mL penicillin/100μg/mL streptomycin (Hyclone, SV30010), and Normocin (Invivogen, ant-nr). Cultures were maintained at 37°C and 5% CO_2. Cultures were passaged with 0.25% Trypsin (Corning, 25–053-CI) when cells reached a density of approximately 500,000 cells/mL and resuspended at densities no lower than 50,000 cells/mL; C) RAW264.7 Murine Macrophages (ATCC, TIB-71) were cultured in non-treated flasks (CellStar, 658195) with DMEM/High Glucose media (Hyclone, SH30243.01) supplemented with with 10% heat-inactivated FBS (Corning, 35011CV), 100 U/mL penicillin/100μg/mL streptomycin (Hyclone, SV30010), and Normocin (Invivogen, ant-nr). Cultures were maintained at 37°C and 5% CO_2. Cells were passaged when they reached a density of approximately 3×10^6 cells/mL using cell scrapers (VWR, 10062–906) to lift cells from flask surface and resuspended at densities of approximately 500,000 cells/mL.

Automated patch clamp.

After isolation, microglia were centrifuged at 380g for 2 min and gently suspended in extracellular solution (in mM: NaCl 140, KCl 5, $CaCl_2$ 2, $MgCl_2$ 1, glucose 5, HEPES 10, pH 7.4 with NaOH) at a concentration of 5×10^6 cells/ml. Automated patch clamp assays were conducted with the IonFlux16 instrument as described previously.[40, 41] Briefly, the IonFlux16 plates consist of 8 patterns, each containing 8 concentration wells: 1 inlet for cell supply, 1 outlet for waste collection, and 2 traps that contain combs that can patch 20 cells per experiment (for a total of 40 cells per pattern). The inlet wells contain intracellular solution (in mM: CsCl 140, CaCl2 1, MgCl2 1, EGTA 11, and HEPES 10, pH 7.2 with

CsOH). The cells were suspended in extracellular solution. The 8 concentration wells contained GABA diluted in extracellular solution. Cells are captured in the traps through a pulse of suction, then whole cell recording access is obtained through a second strong pulse of suction that breaks the membrane. GABA application was achieved by applying pressure onto the appropriate well. Cells are voltage clamped at a holding potential of −80 mV. Current data (n = 16) were normalized in response to maximum current measured with 1 mM GABA and depicted as mean and SEM. EC_{50} values were calculated by non-linear regression.

$GABA_AR$ subunit RT-qPCR.

mRNA was collected from 5×10^6 microglia cells or 23.5 mg of brain tissue from female CFW mice (Charles River, 024CFW) using QIAshredder (Qiagen, 79654) and RNeasy Mini Kit (Qiagen, 74104). Human whole brain RNA was purchased (BioChain, R1434035–50). 50 ng/rxn of microglial mRNA and 10 ng/rxn of whole brain mRNA was analyzed using the QuantiFast SYBR Green RT-PCR kit (Qiagen, 204154) along with the primers listed in the Supporting Information. Data were acquired using an Eppendorf Mastercycler Pro and analyzed by the Delta C_t method. Each measurement was carried out in triplicate. All PCR products were separated with agarose gel electrophoresis (2%) to verify a single band for each primer pair.

Nitric oxide production (Griess assay) and viability assay (CellTiter-Glo).

80 μL of mouse microglia culture (1×10^6 cells/mL) was plated into sterile 384 well plates representing non-activated wells. The remaining culture was activated with 50 ng/mL LPS (Invivogen, NC9836) and 150 U/mL IFNγ (R&D Systems, 485MI100) and distributed into the 384 well plates. 0.1 μL of 800 μM GABA diluted in MilliQ water (final concentration of 1 μM) and appropriate concentrations of compounds of interest diluted in DMSO were added via a TECAN EVO liquid handling system equipped with a 100 nL pin tool (V&P Scientific). Assay plates were incubated for approximately 24 hours (unless otherwise noted) at 37°C, centrifuged, and 40 μL of supernatant transferred to a new plate for analysis using the Griess Assay (Promega, Madison, WI). Absorbance at 530 nm was measured using a TECAN Infinite M1000 plate reader. The remaining 40 μL containing cells was analyzed for toxicity by the CellTiter-Glo Assay (Promega, Madison, WI). Luminescence was read using a TECAN Infinite M1000 plate reader.

Viability assay.

Human liver hepatocellular carcinoma (HEPG2) and human embryonic kidney 293T (HEK293T) cell lines were purchased (ATCC) and cultured in 75 cm^2 flasks (CellStar). Cells were grown in DMEM/High Glucose (Hyclone, #SH3024301) media to which non-essential amino acids (Hyclone, #SH30238.01), 10 mM HEPES (Hyclone, #SH302237.01), 5×10^6 units of penicillin and streptomycin (Hyclone, #SV30010), and 10% of heat inactivated fetal bovine serum (Gibco, #10082147) were added. Cells were harvested using 0.05% Trypsin (Hyclone, #SH3023601), washed with PBS, and dispensed into sterile white, optical bottom 384-well plates (NUNC, #142762). After three hours, small molecule DMSO solutions were transferred with a Tecan Freedom EVO liquid handling system equipped with a 100 nL pin tool (V&P Scientific). The controls were 3-dibutylamino-1-(4-hexyl-phenyl)-

propan-1-one (25 mM in DMSO, positive control) and DMSO (negative control). The cells were incubated for 48 hours followed by the addition of CellTiter-Glo™, a luminescence-based cell viability assay (Promega, Madison, WI). All luminescence readings were performed on a Tecan Infinite M1000 plate reader. The assay was carried out in quadruplet with two independent runs. The data were analyzed by nonlinear regression.

Psychoactive Drug Screening Program.

Detailed protocols for the primary and secondary radioligand binding assays can be found in the National Institute of Mental Health's Psychoactive Drug Screening Program (NIMH PDSP) Assay Protocol Book.[42] Briefly, primary and secondary radioligand binding assays are carried out in a final of volume of 125 µl per well in appropriate binding buffer. The radioactive ligand concentration is close to the Kd. Total binding and nonspecific binding are determined in the absence and presence of 10 µM of appropriate reference compound, respectively. In brief, plates are usually incubated at room temperature and in the dark for 90 min. Reactions are stopped by vacuum filtration onto 0.3% polyethyleneimine (PEI) soaked 96-well filter mats using a 96-well Filtermate harvester, followed by three washes with cold PBS buffer. Scintillation cocktail is then melted onto the microwave-dried filters on a hot plate and radioactivity counted in a Microbeta counter. The data (n = 6) were analyzed by nonlinear regression.

iNOS activity assay.

Mouse microglia were activated with 50 ng/mL LPS (Invivogen, NC9836) and 150 U/mL IFNγ (R&D Systems, 485MI100), and treated with compounds of interest in 6 well plates for 2 or 24 hours. Final DMSO concentrations did not exceed 0.1%. Protein was collected, quantified, and analyzed with the Nitric Oxide Synthase Activity kit (Abcam, ab211083) with minor alterations to the established protocol. Briefly, protein was incubated with cofactors and substrates in 96 well plates for 2.5 hours at 37°C and 5% CO_2. Enhancer was added to each well and incubated for 10 min before Griess reagents were added and incubated. Absorbance at 540 nm was measured using a TECAN Infinite M1000 plate reader. Significance (n = 3) was analyzed by ANOVA.

iNOS RT-qPCR.

1×10^6 mouse microglia cells were plated in 6 well plates (VWR, 10062–892) in 1–2 mL of media, activated with 50 ng/mL LPS (Invivogen, NC9836) and 150 U/mL IFNγ (R&D Systems, 485MI100), and treated with compounds of interest. Final DMSO concentration did not exceed 0.1%. Plates were incubated for stated times at 37°C and 5% CO_2. mRNA was collected using QIAshredder (Qiagen, 79654) and RNeasy Mini Kit (Qiagen, 74104). mRNA was analyzed using the QuantiFast SYBR Green RT-PCR kit (Qiagen, 204154) along with iNOS primers (F: 5' – ACA TCA GGT CGG CCA TCA CT – 3', R: 5' – CGT ACC GGA TGA GCT GTG AAT – 3'). Expected product size was 87 bp. Data were acquired using an Eppendorf Mastercycler Pro and analyzed by the Delta C_t method. Each measurement was carried out in triplicate and significance analyzed by ANOVA. All PCR products were separated with agarose gel electrophoresis (2%) to verify a single band for each primer pair.

iNOS ELISA.

Mouse microglia (2 mL of 500,000 cells/mL cell solution) were activated with 50 ng/mL LPS (Invivogen, NC9836) and 150 U/mL IFNγ (R&D Systems, 485MI100), and treated with compounds of interest in 6 well plates (VWR, 10062–892) for 24 hours. Final DMSO concentrations did not exceed 0.1%. Cells were lysed with RIPA buffer and protein concentration quantified with the Pierce Rapid Gold BCA Protein Assay Kit (Thermo Scientific, A53227). Samples at 50 μg/mL were analyzed with the Mouse iNOS ELISA kit (ABCAM, ab253219). Absorbance (λ: 450 nm) was measured using a TECAN Infinite M1000 plate reader. Each measurement was carried with an n = 3 and significance analyzed by ANOVA.

Formalin test.

GL-IV-03 and ketoprofen was formulated in 2.5% polyethylene glycol and 2% hydroxypropyl methylcellulose. Each treatment was administered over a period of four days by oral gavage at 10 mL/kg once a day. Twenty minutes after the administration, 20 μL of 2% formalin in 0.9% saline solution was administered to the right hind paw via intraplantar injection while restrained. Immediately after the hind paw injection, mice were removed and placed into the observation chamber for 5 minutes to measure Phase I behavior, representing acute peripheral pain mediated by direct activation of nociceptors.[28] The animal was observed in 5 seconds intervals and occurrence of licking and biting the injected paw was recorded to determine to a pain score of 3 as defined in the Dubuisson and Dennis Model.[43] Mice were placed back in their home cage for a 15 minute quiescent period and reanalyzed for 5 minutes to measure Phase II behavior, representative of an inflammatory and/or neurogenic response.[28] The group size was six and unpaired t-test was used to determine significance in comparison to the vehicle group.

Rotarod test:

Female Swiss Webster mice were trained to maintain balance at a constant speed of 15 rpm on the rotarod apparatus (Omnitech Electronics Inc., Nova Scotia, Canada) until mice could perform for three minutes at three consecutive time points. Separate groups of mice (n = 10) received intraperitoneal (i.p.) injections of compounds (10% DMSO, 40% propylene glycol and 50% PBS) at 5 mL/kg or orally administrated compounds (2.5% polyethylene glycol and 2% hydroxypropyl methylcellulose) at 10 mL/kg. 10, 30 and 60 min after each injection, mice were placed on the rotarod for 3 min. If a mouse fell before the three minutes were completed, it was placed again on the rod. If a mouse fell for the second time, the time of the fall was recorded. Significance was calculated by 2way ANOVA.

Supplementary Material

Refer to Web version on PubMed Central for supplementary material.

Acknowledgement

We thank Dr. Beryl R. Forman and Jennifer L. Nemke (Animal Resource Center at UWM) for their guidance and support. This work was supported by the National Institutes of Health (USA) R41HL147658 (L.A.A. and D.C.S.), R01NS076517 (J.M.C. and L.A.A.) and R01HL118561 (J.M.C., L.A.A., and D.C.S.), as well as the University of

Wisconsin-Milwaukee, University of Wisconsin-Milwaukee Research Foundation (Catalyst grant), the Lynde and Harry Bradley Foundation, and the Richard and Ethel Herzfeld Foundation. In addition, this work was supported by grant CHE-1625735 from the National Science Foundation, Division of Chemistry.

References

1. Hedegaard H, Warner M, and Minino AM (2017) Drug Overdose Deaths in the United States, 1999–2016. NCHS Data Brief, No. 294, 1–8.
2. van Hecke O, Austin SK, Khan RA, Smith BH, and Torrance N. (2014) Neuropathic pain in the general population: a systematic review of epidemiological studies. Pain 155, 654–662. [PubMed: 24291734]
3. Rock RB, Gekker G, Hu S, Sheng WS, Cheeran M, Lokensgard JR, and Peterson PK (2004) Role of microglia in central nervous system infections. Clin. Microbiol. Rev 17, 942–964. [PubMed: 15489356]
4. Jakel S, and Dimou L. (2017) Glial Cells and Their Function in the Adult Brain: A Journey through the History of Their Ablation. Front. Cell. Neurosci 11, 24. [PubMed: 28243193]
5. Salter MW, and Stevens B. (2017) Microglia emerge as central players in brain disease. Nat. Med 23, 1018–1027. [PubMed: 28886007]
6. Shinozaki Y, Nomura M, Iwatsuki K, Moriyama Y, Gachet C, and Koizumi S. (2014) Microglia trigger astrocyte-mediated neuroprotection via purinergic gliotransmission. Sci. Rep 4, 4329. [PubMed: 24710318]
7. Moller T. (2002) Calcium signaling in microglial cells. Glia 40, 184–194. [PubMed: 12379906]
8. Mika J, Zychowska M, Popiolek-Barczyk K, Rojewska E, and Przewlocka B. (2013) Importance of glial activation in neuropathic pain. Eur. J. Pharmacol 716, 106–119. [PubMed: 23500198]
9. Inoue K. (2017) Purinergic signaling in microglia in the pathogenesis of neuropathic pain. Proc. Jpn. Acad. Ser. B Phys. Biol. Sci 93, 174–182.
10. Donnelly-Roberts D, McGaraughty S, Shieh CC, Honore P, and Jarvis MF (2008) Painful purinergic receptors. J. Pharmacol. Exp. Ther 324, 409–415. [PubMed: 18042830]
11. Levy D, and Zochodne DW (2004) NO pain: potential roles of nitric oxide in neuropathic pain. Pain Pract. 4, 11–18. [PubMed: 17129298]
12. Forstermann U, and Sessa WC (2012) Nitric oxide synthases: regulation and function. Eur. Heart J 33, 829–837. [PubMed: 21890489]
13. Sierra A, Navascues J, Cuadros MA, Calvente R, Martin-Oliva D, Ferrer-Martin RM, Martin-Estebane M, Carrasco MC, and Marin-Teva JL (2014) Expression of inducible nitric oxide synthase (iNOS) in microglia of the developing quail retina. PLoS One 9, e106048.
14. Lee M, Schwab C, and McGeer PL (2011) Astrocytes are GABAergic cells that modulate microglial activity. Glia 59, 152–165. [PubMed: 21046567]
15. Olsen RW, and Sieghart W. (2008) International Union of Pharmacology. LXX. Subtypes of gamma-aminobutyric acid(A) receptors: classification on the basis of subunit composition, pharmacology, and function. Update. Pharmacol. Rev 60, 243–260. [PubMed: 18790874]
16. Mortensen M, Patel B, and Smart TG (2011) GABA Potency at GABA(A) Receptors Found in Synaptic and Extrasynaptic Zones. Front. Cell. Neurosci 6, 1–10. [PubMed: 22319471]
17. Connolly CN, Krishek BJ, McDonald BJ, Smart TG, and Moss SJ (1996) Assembly and cell surface expression of heteromeric and homomeric gamma-aminobutyric acid type A receptors. J. Biol. Chem 271, 89–96. [PubMed: 8550630]
18. Wu C, Qin X, Du H, Li N, Ren W, and Peng Y. (2017) The immunological function of GABAergic system. Front Biosci-Landmrk 22, 1162–1172.
19. Forkuo GS, Nieman AN, Yuan NY, Kodali R, Yu OB, Zahn NM, Jahan R, Li G, Stephen MR, Guthrie ML, Poe MM, Hartzler BD, Harris TW, Yocum GT, Emala CW, Steeber DA, Stafford DC, Cook JM, and Arnold LA (2017) Alleviation of Multiple Asthmatic Pathologic Features with Orally Available and Subtype Selective GABAA Receptor Modulators. Mol. Pharm 14, 2088–2098. [PubMed: 28440659]
20. Forkuo GS, Nieman AN, Kodali R, Zahn NM, Li G, Rashid Roni MS, Stephen MR, Harris TW, Jahan R, Guthrie ML, Yu OB, Fisher JL, Yocum GT, Emala CW, Steeber DA, Stafford DC, Cook

JM, and Arnold LA (2018) A Novel Orally Available Asthma Drug Candidate That Reduces Smooth Muscle Constriction and Inflammation by Targeting GABAA Receptors in the Lung. Mol. Pharm 15, 1766–1777. [PubMed: 29578347]

21. Hoeffel G, and Ginhoux F. (2015) Ontogeny of Tissue-Resident Macrophages. Front. Immunol 6, 486. [PubMed: 26441990]
22. Di Lio A, Benke D, Besson M, Desmeules J, Daali Y, Wang ZJ, Edwankar R, Cook JM, and Zeilhofer HU (2011) HZ166, a novel GABAA receptor subtype-selective benzodiazepine site ligand, is antihyperalgesic in mouse models of inflammatory and neuropathic pain. Neuropharmacology 60, 626–632. [PubMed: 21145329]
23. Lewter LA, Fisher JL, Siemian JN, Methuku KR, Poe MM, Cook JM, and Li JX (2017) Antinociceptive Effects of a Novel alpha2/alpha3-Subtype Selective GABAA Receptor Positive Allosteric Modulator. ACS Chem. Neurosci 8, 1305–1312. [PubMed: 28150939]
24. Garcia-Mesa Y, Jay TR, Checkley MA, Luttge B, Dobrowolski C, Valadkhan S, Landreth GE, Karn J, and Alvarez-Carbonell D. (2017) Immortalization of primary microglia: a new platform to study HIV regulation in the central nervous system. J. Neurovirol 23, 47–66. [PubMed: 27873219]
25. Besnard J, Ruda GF, Setola V, Abecassis K, Rodriguiz RM, Huang XP, Norval S, Sassano MF, Shin AI, Webster LA, Simeons FR, Stojanovski L, Prat A, Seidah NG, Constam DB, Bickerton GR, Read KD, Wetsel WC, Gilbert IH, Roth BL, and Hopkins AL (2012) Automated design of ligands to polypharmacological profiles. Nature 492, 215–220. [PubMed: 23235874]
26. Ghelardini C, Galeotti N, and Bartolini A. (2000) Pharmacological identification of SM-21, the novel sigma(2) antagonist. Pharmacol. Biochem. Behav 67, 659–662. [PubMed: 11164098]
27. Kamei J, and Nagase H. (2001) Norbinaltorphimine, a selective kappa-opioid receptor antagonist, induces an itch-associated response in mice. Eur. J. Pharmacol 418, 141–145. [PubMed: 11334876]
28. Abbott FV, Franklin KB, and Westbrook RF (1995) The formalin test: scoring properties of the first and second phases of the pain response in rats. Pain 60, 91–102. [PubMed: 7715946]
29. Ji RR, Berta T, and Nedergaard M. (2013) Glia and pain: is chronic pain a gliopathy? Pain 154 Suppl 1, S10–28. [PubMed: 23792284]
30. Romer D, Buscher HH, Hill RC, Maurer R, Petcher TJ, Zeugner H, Benson W, Finner E, Milkowski W, and Thies PW (1982) Unexpected opioid activity in a known class of drug. Life Sci. 31, 1217–1220. [PubMed: 6292610]
31. Anzini M, Canullo L, Braile C, Cappelli A, Gallelli A, Vomero S, Menziani MC, De Benedetti PG, Rizzo M, Collina S, Azzolina O, Sbacchi M, Ghelardini C, and Galeotti N. (2003) Synthesis, biological evaluation, and receptor docking simulations of 2-[(acylamino)ethyl]-1,4-benzodiazepines as kappa-opioid receptor agonists endowed with antinociceptive and antiamnesic activity. J. Med. Chem 46, 3853–3864. [PubMed: 12930147]
32. Cappelli A, Anzini M, Vomero S, Menziani MC, De Benedetti PG, Sbacchi M, Clarke GD, and Mennuni L. (1996) Synthesis, biological evaluation, and quantitative receptor docking simulations of 2-[(acylamino)ethyl]-1,4-benzodiazepines as novel tifluadom-like ligands with high affinity and selectivity for kappa-opioid receptors. J. Med. Chem 39, 860–872. [PubMed: 8632410]
33. Cox RF, and Collins MA (2001) The effects of benzodiazepines on human opioid receptor binding and function. Anesth. Analg 93, 354–358. [PubMed: 11473860]
34. Chao CC, Gekker G, Hu S, Sheng WS, Shark KB, Bu DF, Archer S, Bidlack JM, and Peterson PK (1996) kappa opioid receptors in human microglia downregulate human immunodeficiency virus 1 expression. Proc. Natl. Acad. Sci. U. S. A 93, 8051–8056. [PubMed: 8755601]
35. Mika J, Popiolek-Barczyk K, Rojewska E, Makuch W, Starowicz K, and Przewlocka B. (2014) Delta-opioid receptor analgesia is independent of microglial activation in a rat model of neuropathic pain. PLoS One 9, e104420.
36. Popiolek-Barczyk K, Piotrowska A, Makuch W, and Mika J. (2017) Biphalin, a Dimeric Enkephalin, Alleviates LPS-Induced Activation in Rat Primary Microglial Cultures in Opioid Receptor-Dependent and Receptor-Independent Manners. Neural Plast. 2017, 3829472.
37. Nozaki-Taguchi N, and Yamamoto T. (1998) Involvement of nitric oxide in peripheral antinociception mediated by kappa- and delta-opioid receptors. Anesth. Analg 87, 388–393. [PubMed: 9706936]

38. Obara I, Parkitna JR, Korostynski M, Makuch W, Kaminska D, Przewlocka B, and Przewlocki R. (2009) Local peripheral opioid effects and expression of opioid genes in the spinal cord and dorsal root ganglia in neuropathic and inflammatory pain. Pain 141, 283–291. [PubMed: 19147290]

39. Gallantine EL, and Meert TF (2008) Antinociceptive and adverse effects of mu- and kappa-opioid receptor agonists: a comparison of morphine and U50488-H. Basic Clin. Pharmacol. Toxicol 103, 419–427. [PubMed: 18699797]

40. Yuan NY, Poe MM, Witzigmann C, Cook JM, Stafford D, and Arnold LA (2016) Characterization of GABAA receptor ligands with automated patch-clamp using human neurons derived from pluripotent stem cells. J. Pharmacol. Toxicol. Methods 82, 109–114. [PubMed: 27544543]

41. Chen Q, Yim PD, Yuan N, Johnson J, Cook JM, Smith S, Ionescu-Zanetti C, Wang ZJ, Arnold LA, and Emala CW (2012) Comparison of cell expression formats for the characterization of GABA(A) channels using a microfluidic patch clamp system. Assay Drug Dev. Technol 10, 325–335. [PubMed: 22574655]

42. Roth B. (2018) National Institute of Mental Health Psychoactive Drug Screening Program, In Assay Protocol Book, p 359, Department of Pharmacology, University of North Carolina at Chapel Hill.

43. Dubuisson D, and Dennis SG (1977) The formalin test: a quantitative study of the analgesic effects of morphine, meperidine, and brain stem stimulation in rats and cats. Pain 4, 161–174. [PubMed: 564014]

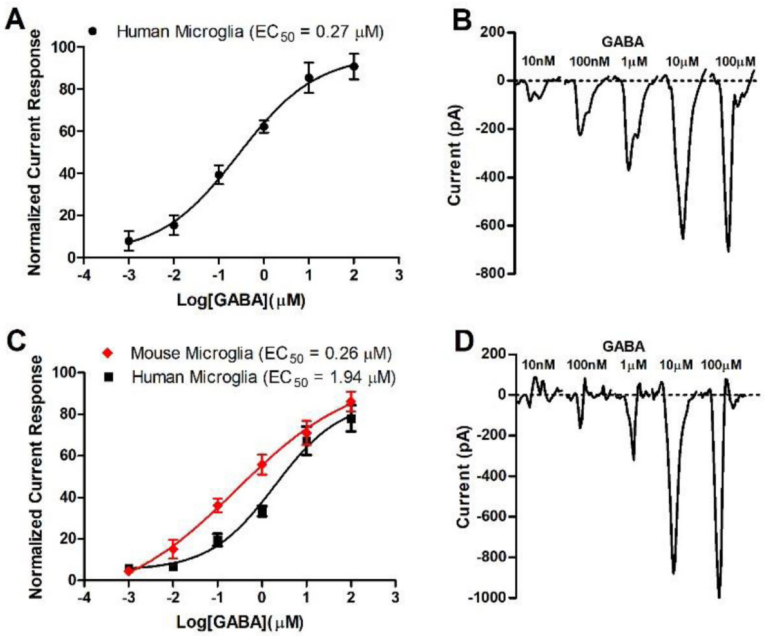

Figure 1.

Electrophysiology measurement (patch clamp). A) Current response with HMC3 human microglia cells. Data (n = 12) were normalized in response to maximum current measured with 1 mM GABA and depicted as mean and SEM. EC_{50} was calculated by non-linear regression; B) 10 second average current sweeps of increasing concentrations of GABA with HMC3 cells; C) Current response with immortalized human and mouse microglia cells.[24] Data (n = 16) were normalized in response to maximum current measured with 1 mM GABA and depicted as mean and SEM. D) 10 second average current sweeps of increasing concentrations of GABA with immortalized human microglia cells. EC_{50} values were calculated by non-linear regression.

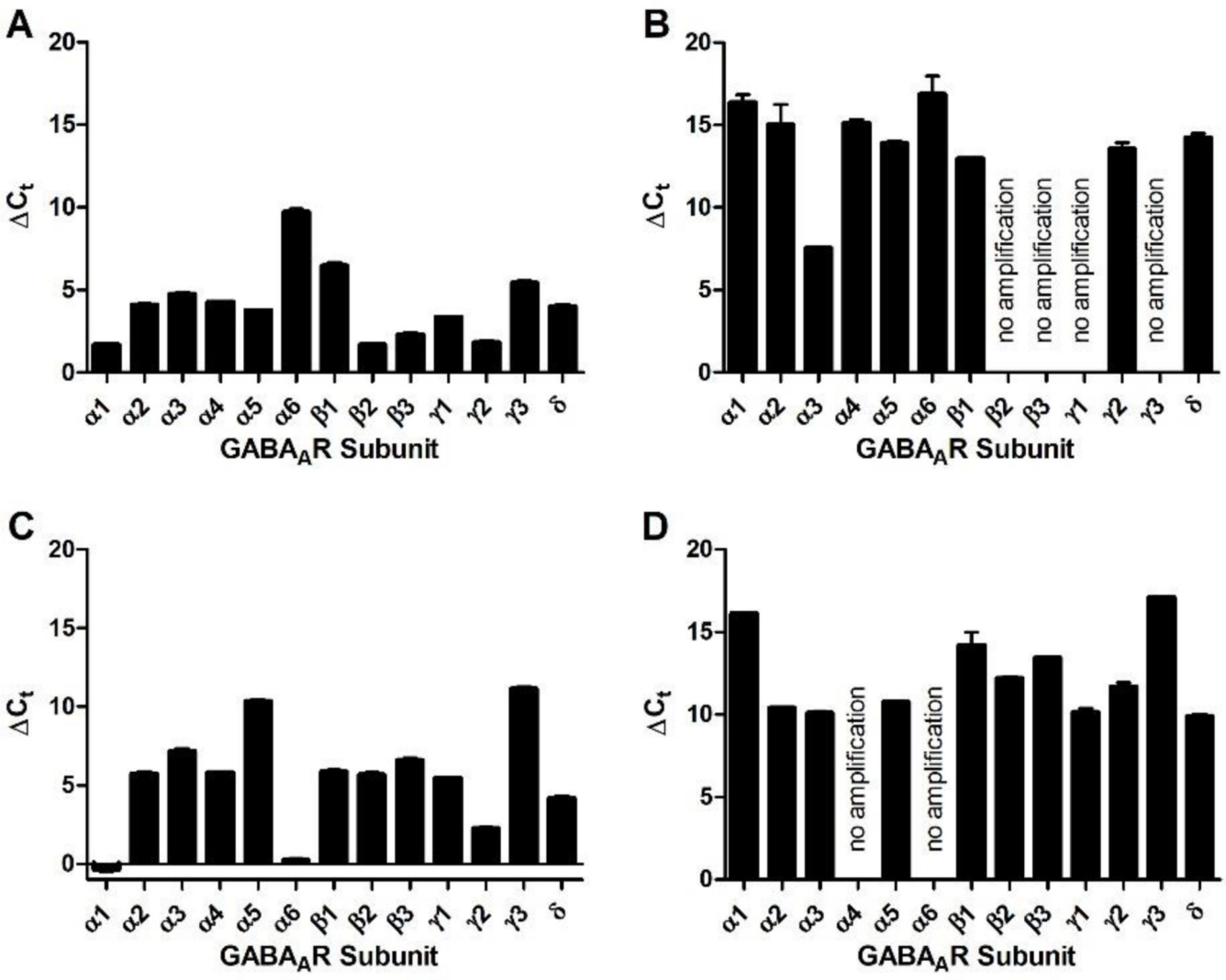

Figure 2.

Expression of GABA$_A$R subunit mRNA isolated from immortalized human and mouse microglia. mRNA (10 ng for brain extracts and 50 ng for microglia) was amplified with a QuantiFast SYBR green RT-qPCR kit (Quiagen) and cycle numbers for each subunit were normalized to GAPDH using the ΔCt method (n = 3). A) human brain extract, B) human microglia, C) mouse cerebellum extract, and D) mouse microglia.

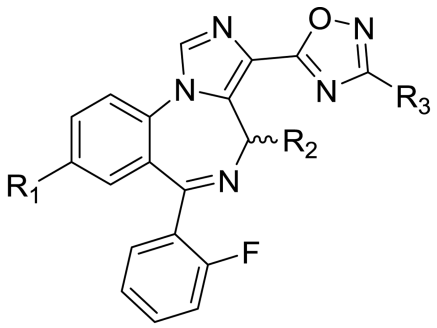

R_1 = C≡CH
R_2 = (S)CH3
R_3 = CH_3 (**GL-I-65**)
CH_2CH_3 (**GL-I-66**)
$CH(CH_3)_2$ (**GL-I-81**)

R_1 = Br
R_2 = (R)CH3
R_3 = CH_3 (**GL-III-60**)
CH_2CH_3 (**GL-III-98**)
$CH(CH_3)_2$ (**GL-IV-01**)

R_1 = cyclopropyl
R_2 = (R)CH3
R_3 = CH_3 (**GL-III-63**)
CH_2CH_3 (**GL-IV-03**)
$CH(CH_3)_2$ (**GL-IV-04**)

R_1 = C≡CH
R_2 = (R)CH3
R_3 = CH_3 (**MP-IV-004**)
CH_2CH_3 (**MP-IV-005**)
$CH(CH_3)_2$ (**MP-IV-010**)

Figure 3.
Chemical structures of MP-IV-010, GL-IV-03, and related compounds.

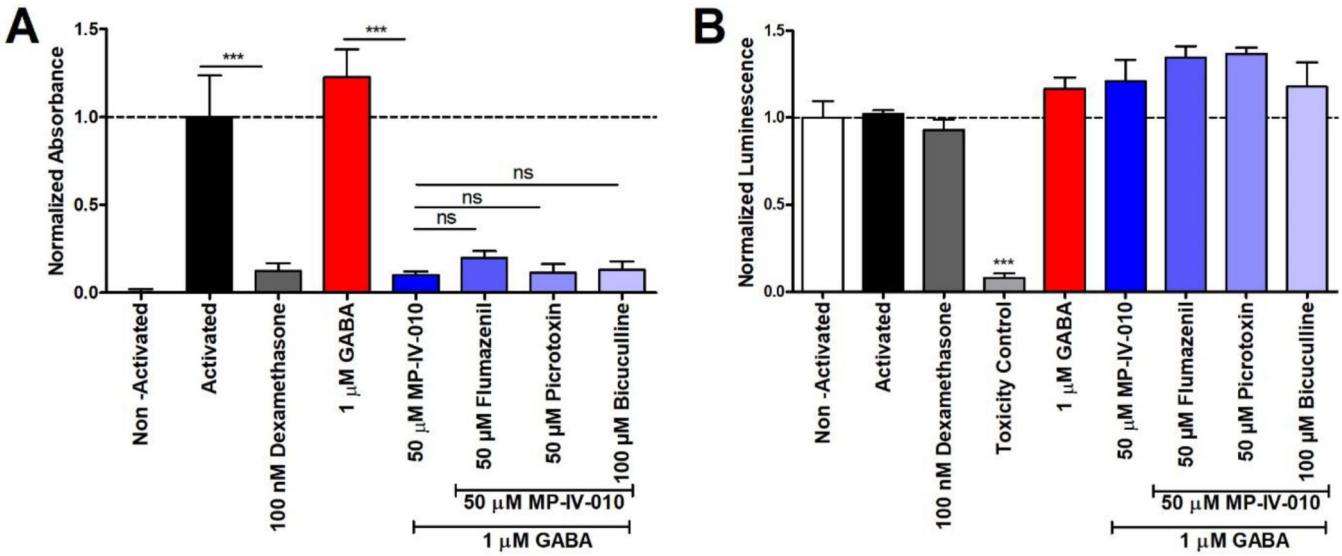

Figure 4.

Reduction of NO in the presence of MP-IV-010 and $GABA_AR$ receptor antagonists. A) Mouse microglia were activated with LPS/IFNγ and treated with indicated compound combinations. NO levels of the media were quantified with a Griess assay after 14 h. B) ATP levels of cells were quantified with CellTiter-Glo. Data are presented as mean and SEM (n = 8). *** indicate $p < 0.001$, ns is no significance. (ANOVA)

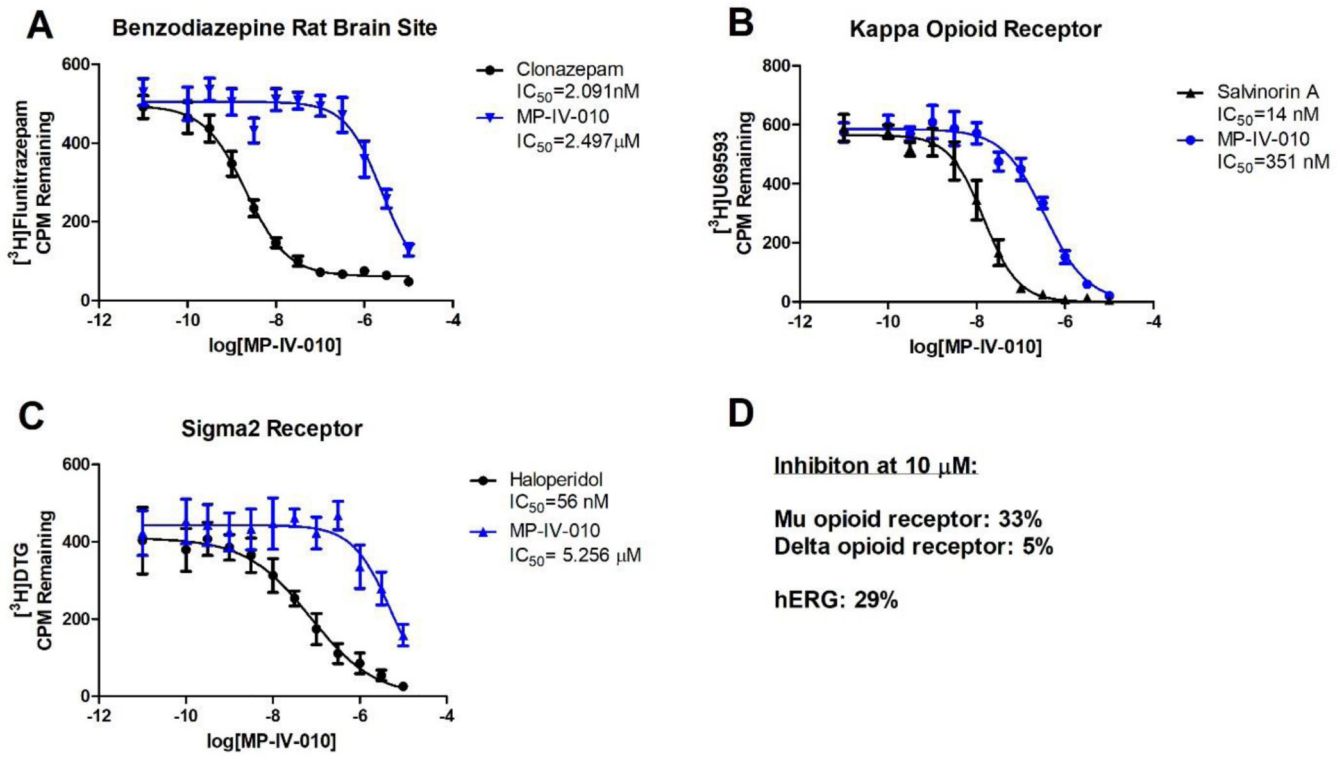

Figure 5.

Concentration-dependent receptor binding assays for MP-IV-010. A) $GABA_AR$; rat brain homogenate was incubated with ^{3}H-flunitrazepam; B) κ-opioid receptor; cell lysate from stably transfected HEK cells was incubated with ^{3}H-U69593; C) σ2 receptor; cell lysate from stably transfected HEK cells was incubated ^{3}H-ditolylguanidine. (n = 6); D) Inhibition at 10 μM MP-IV-010: μ-opioid receptor; cell lysate from stably transfected HEK cells was incubated with ^{3}H-DADLE; δ-opioid receptor; cell lysate from stably transfected HEK cells was incubated with ^{3}H-DAMGO; hERG; cell lysate from stably transfected HEK cells was incubated with ^{3}H-dofetilide. Data are presented as mean and SEM (n = 8). Non-linear regression was used to determine IC_{50} values.

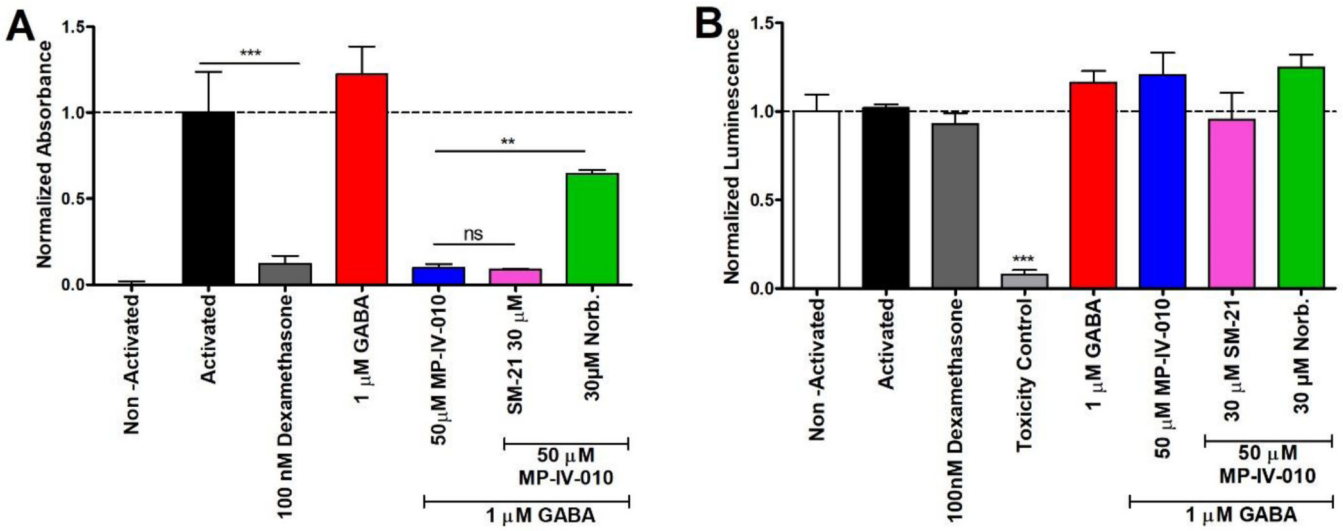

Figure 6.

Reduction of NO in the presence of MP-IV-010 and receptor antagonists. A) Mouse microglia were activated with LPS/IFNγ and treated with indicated compound combinations. NO levels of the media were quantified with a Griess assay after 14 h. B) ATP levels of cells were quantified with CellTiter-Glo. Data are presented as mean and SEM (n = 8). ** and *** indicate $p < 0.01$ and $p < 0.001$, ns is no significance. (ANOVA)

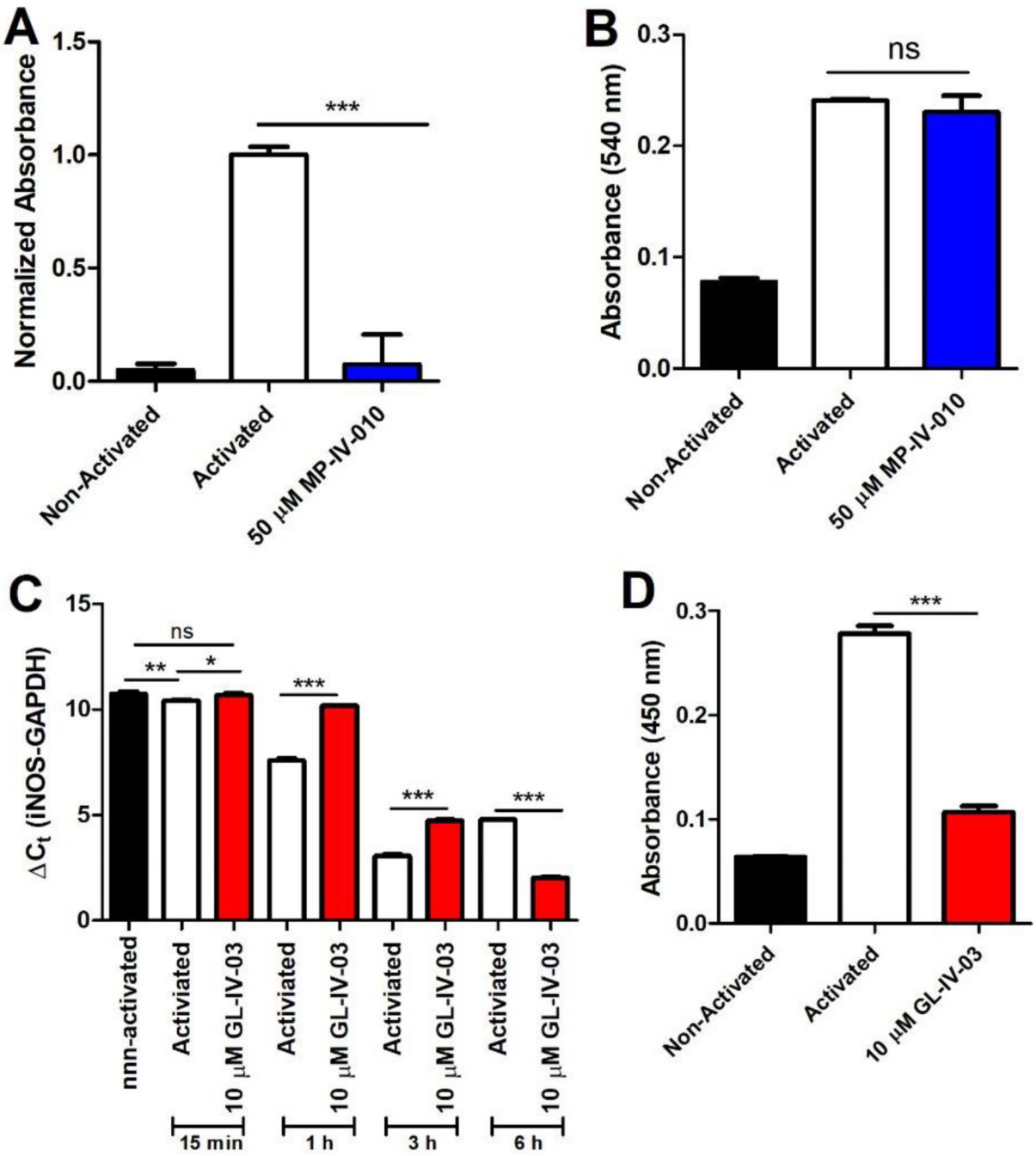

Figure 7.

Measurement of iNOS mRNA, protein, and activity in activated and non-activated mouse microglia treated with vehicle or MP-IV-010 or GL-IV-03. A) Cellular proteins were isolated from mouse microglia treated with vehicle and mouse microglia activated with IFNγ/LPS and treated for 24 hours with vehicle or 50 μM MP-IV-010. Specific iNOS activity was determined with an Abcam iNOS Activity Assay kit (n = 4); B) Cellular proteins were isolated from mouse microglia and mouse microglia activated for 24 hours with IFNγ/LPS. Cellular proteins from activated microglia were treated for 2 hours with 50 μM MP-IV-010

and iNOS activity was determined for all protein extracts with an Abcam iNOS Activity Assay kit (n =3); C) Mouse microglia were activated with IFNγ/LPS and treated with vehicle or 10 μM GL-IV-03. mRNA was isolated after 15 min, 1 h, 3 h and 6 h and *iNOS* was quantified using RT-qPCR. Cycle numbers for each sample were normalized to GAPDH using the ΔCt method (n = 3). Mouse microglia were activated with IFNγ/LPS and treated with vehicle or 10 μM GL-IV-03 for 24 h. Cellular protein was extracted and analyzed with the Mouse iNOS ELISA kit from Abcam (n =3). *, ($p < 0.05$), ** ($p < 0.01$) or *** ($p < 0.001$) significance was calculate with ANOVA.

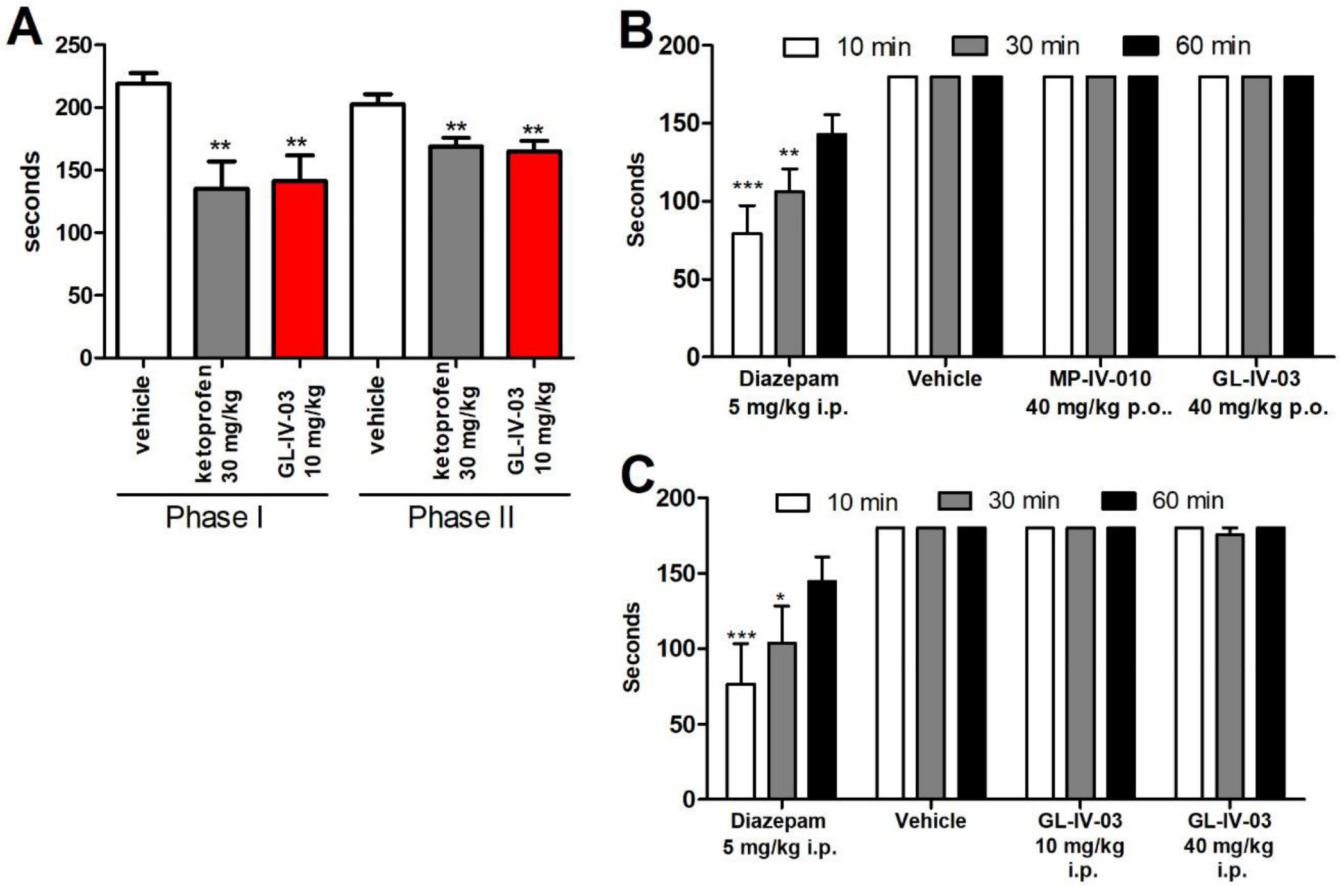

Figure 8.

In vivo evaluation of MP-IV-010 and GL-IV-03. A) Formalin test: Swiss Webster mice were treated orally four days in advance with indicated compounds and doses before the injection of 2% formalin in the right hind paw. Mice were evaluated during the first 5 min (phase 1) and after 20 minutes (phase 2) for 5 minutes in 5 seconds intervals. Licking and biting the right hind paw during a 5 second interval was noted and combined as total time addressing the injected paw. Data is given as mean with SEM (n = 8). ** indicate $p < 0.01$ (unpaired t-test); B) and C) Sensorimotor coordination: Swiss Webster mice were tested on a rotarod at 15 rpm for 3 min at 10, 30, and 60 min following compound treatment at indicated dose and administration. The time of fall was recorded if it occurred prior to 3 min. Data are expressed as mean ± SEM (n = 10). *, ($p < 0.05$), ** ($p < 0.01$) or *** ($p < 0.001$) significance compared to vehicle-treated mice (2 way ANOVA).

Table 1.

$GABA_AR$ ligand induced NO inhibition and cytotoxicity

	Inhibition of NO production (%)				Cell viability (%)			
	RAW macrophages		Mouse microglia		RAW macrophages	Mouse microglia	HEK293[b]	HEPG2[b]
Compound[a]	50 μM	10 μM	50 μM	10 μM	50 μM	50 μM	120 μM	120 μM
GL-I-48		4 ± 2		0 ± 4	100 ± 12	78 ± 5	65 ± 8	100 ± 4
GL-I-50		0 ± 1		33 ± 6	100 ± 9	88 ± 9	97 ± 12	100 ± 2
GL-I-62		3 ± 2		13 ± 7	100 ± 3	92 ± 7	79 ± 7	89 ± 10
GL-I-64		3 ± 3		24 ± 3	100 ± 5	81 ± 5	77 ± 13	100 ± 9
GL-I-65			19 ± 9			100 ± 12		
GL-I-66			86 ± 11	5 ± 2		71 ± 9		
GL-I-81	6 ± 2	0 ± 2	87 ± 2	64 ± 9	91 ± 7	94 ± 10		
GL-II-05		0 ± 1		12 ± 5	100 ± 11	88 ± 8	94 ± 3	92 ± 5
GL-II-06		4 ± 2		14 ± 3	100 ± 10	87 ± 13	83 ± 13	89 ± 5
GL-II-18		11 ± 4		49 ± 10	99 ± 2	89 ± 9	53 ± 10	100 ± 8
GL-II-19		2 ± 2		32 ± 4		100 ± 11	90 ± 5	100 ± 9
GL-II-32		6 ± 3		7 ± 2	100 ± 4	95 ± 8	80 ± 6	
GL-II-33			0 ± 3		100 ± 7	100 ± 4		
GL-II-51		0 ± 1		9 ± 4	100 ± 3	95 ± 2	91 ± 4	100 ± 16
GL-II-54			0 ± 4		100 ± 8	95 ± 3		
GL-II-61		10 ± 4		28 ± 2	100 ± 8	91 ± 8	83 ± 10	82 ± 3
GL-II-79		0 ± 3		44 ± 6	100 ± 3	84 ± 5	91 ± 13	100 ± 7
GL-II-80		5 ± 3		38 ± 8	100 ± 2	85 ± 1	76 ± 8	100 ± 9
GL-III-13		0 ± 2			100 ± 9	92 ± 9	74 ± 5	100 ± 10
GL-III-23			28 ± 5			100 ± 2	65 ± 5	90 ± 13
GL-III-24		68 ± 8		67 ± 12	100 ± 12	98 ± 5	78 ± 6	91 ± 12
GL-III-25		38 ± 9		25 ± 10	100 ± 8	98 ± 4	93 ± 4	100 ± 5
GL-III-27		1 ± 3		29 ± 8	100 ± 4	86 ± 8	91 ± 2	77 ± 7
GL-III-35		0 ± 4		17 ± 7	100 ± 2	100 ± 8	79 ± 8	98 ± 8
GL-III-36	58 ± 9	0 ± 3	41 ± 7	8 ± 5	81 ± 5	97 ± 9	80 ± 9	100 ± 9
GL-III-42		0 ± 5		55 ± 12	100 ± 6	82 ± 10	62 ± 11	100 ± 8
GL-III-52		2 ± 2		57 ± 11	97 ± 8	85 ± 8	73 ± 8	81 ± 9
GL-III-53		3 ± 2		85 ± 14	97 ± 7	72 ± 7	47 ± 10	94 ± 10
GL-III-54		6 ± 4		31 ± 9	99 ± 12	82 ± 6	96 ± 12	93 ± 4
GL-III-58		3 ± 1		48 ± 4	100 ± 14	83 ± 4	89 ± 2	100 ± 5
GL-III-59		8 ± 1		43 ± 7	100 ± 3	96 ± 4	100 ± 4	100 ± 2
GL-III-60	39 ± 8	0 ± 1	68 ± 8	55 ± 8	86 ± 12	100 ± 9	64 ± 6	100 ± 11
GL-III-63	62 ± 12	13 ± 4	89 ± 12	25 ± 4	87 ± 15	100 ± 8	18 ± 4	16 ± 6
GL-III-64			26 ± 10			96 ± 10	75 ± 8	75 ± 10

	Inhibition of NO production (%)				Cell viability (%)			
	RAW macrophages		Mouse microglia		RAW macrophages	Mouse microglia	HEK293[b]	HEPG2[b]
GL-III-66		6 ± 4		13 ± 2	100 ± 9	85 ± 15	46 ± 4	86 ± 8
GL-III-67		4 ± 2		33 ± 1	100 ± 7	85 ± 10	66 ± 6	100 ± 9
GL-III-68		5 ± 1		24 ± 5	100 ± 8	83 ± 3	56 ± 11	83 ± 2
GL-III-69		0 ± 1		37 ± 6	98 ± 10	87 ± 6	73 ± 10	88 ± 5
GL-III-70		2 ± 2		32 ± 4	100 ± 2	86 ± 2	86 ± 12	100 ± 5
GL-III-72		57 ± 7		21 ± 7	77 ± 4	100 ± 10	64 ± 8	100 ± 3
GL-III-73		1 ± 6		40 ± 3	100 ± 4	80 ± 9	86 ± 6	100 ± 9
GL-III-75		3 ± 5		44 ± 2	100 ± 2	87 ± 7	73 ± 2	74 ± 6
GL-III-76		0 ± 3		34 ± 1	100 ± 5	80 ± 2	59 ± 4	90 ± 6
GL-III-76A		6 ± 3		58 ± 9	97 ± 4	100 ± 9	0 ± 3	0 ± 2
GL-III-77		29 ± 2		31 ± 2	85 ± 3	98 ± 4	0 ± 2	0 ± 4
GL-III-78		0 ± 6		39 ± 5	97 ± 2	79 ± 6	56 ± 8	100 ± 15
GL-III-84		10 ± 5		32 ± 4	100 ± 12	96 ± 8	64 ± 5	100 ± 10
GL-III-85		0 ± 2		34 ± 8	100 ± 10	84 ± 12	70 ± 12	100 ± 11
GL-III-86		7 ± 4		39 ± 7	100 ± 14	99 ± 15	66 ± 10	100 ± 8
GL-III-87		0 ± 1		23 ± 7	100 ± 7	100 ± 2	90 ± 10	100 ± 5
GL-III-97		6 ± 1		11 ± 6	98 ± 3	100 ± 4	54 ± 9	100 ± 12
GL-III-98		1 ± 4		75 ± 9	100 ± 11	83 ± 6	42 ± 8	56 ± 5
GL-III-99		19 ± 3		49 ± 5	100 ± 9	95 ± 9	87 ± 11	93 ± 7
GL-IV-01		17 ± 7		56 ± 11	100 ± 9	100 ± 9	72 ± 8	100 ± 9
GL-IV-03		75 ± 12		90 ± 10	97 ± 7	100 ± 5	47 ± 5	39 ± 5
GL-IV-04		11 ± 2		62 ± 8	100 ± 7	86 ± 6	71 ± 6	100 ± 6
GL-IV-05		14 ± 3		59 ± 4	100 ± 6	88 ± 12	47 ± 3	100 ± 10
GL-IV-17		5 ± 5		41 ± 5	100 ± 5	89 ± 9	67 ± 5	93 ± 8
GL-IV-18		10 ± 7		63 ± 9	98 ± 5	81 ± 10	88 ± 5	80 ± 14
DMH-D-053		13 ± 2			100 ± 8	93 ± 13	97 ± 10	100 ± 11
KRM-II-18B			0 ± 1			100 ± 3		
KRM-II-81			0 ± 1			100 ± 5	96 ± 11	100 ± 12
KRM-II-82			0 ± 3			100 ± 6		
MP-III-022	51 ± 7	9 ± 5	60 ± 12	36 ± 6	100 ± 11	86 ± 2	75 ± 13	94 ± 7
MP-III-080			0 ± 3			100 ± 14		
MP-IV-004	51 ± 7	0 ± 1	60 ± 6	34 ± 5	83 ± 12	100 ± 5	40 ± 8	100 ± 4
MP-IV-005	59 ± 9	5 ± 3	89 ± 17	45 ± 3	86 ± 14	86 ± 13	68 ± 14	98 ± 8
MP-IV-010	63 ± 11	10 ± 2	96 ± 13	66 ± 13	81 ± 10	91 ± 10	41 ± 4	45 ± 7
QH-II-66		17 ± 6		54 ± 9	100 ± 12	97 ± 11	81 ± 2	100 ± 4
YT-III-271			0 ± 4			100 ± 3		
YT-III-31			0 ± 2			100 ± 8	96 ± 10	100 ± 7

[a]Structures are depicted in Supporting Information,

[b] concentration response curves are depicted in Supporting Information